PCCP

Accepted Manuscript

ROYAL SOCIETY OF CHEMISTRY

www.rsc.org/pccp

Journal Name

RSCPublishing

ARTICLE

SF_6^- Photodetachment near the Adiabatic Limit

I. Luzon[a], M. Nagler[a], O. Heber[b], D. Strasser[a]

Cite this: DOI: 10.1039/xoxxoooooox

Received ooth January 2012,
Accepted ooth January 2012

DOI: 10.1039/xoxxoooooox

www.rsc.org/

High sensitivity photodetachment cross-section measurements of SF_6^- are performed near the adiabatic threshold limit. The extraction of adiabatic detachment energy (ADE) from the high sensitivity measurement of cross section change as a function of photon energy is discussed. Below the vertical detachment energy a steep 4 orders of magnitude cross section drop is observed, with cross sections as low as $2 \cdot 10^{-6}$Å^2 measured for photon energies below 2eV. The cross-section is fitted with both the expected spectral shape based on recently calculated Frank-Condon overlaps as well as with a phenomenological threshold function. The resulting 1.7 ± 0.02 eV ADE values are significantly higher than previously recommended experimental ADE values obtained based on kinetics modeling, possible differences between the experimental approaches are discussed.

Introduction

In the last decade Sulfur hexafluoride (SF_6) has attracted considerable scientific attention due to its role as electron scavenger in various industrial applications[1], its increasing importance to global warming[2–5] as well as fundamental research interests[1,6–12]. Nevertheless, basic questions about the attachment of electrons to neutral SF_6 and the detachment of electrons from the anion system remain only partially resolved and subject of ongoing research,[8–11,13–15] One of the ongoing debates concerns the adiabatic detachment energy (ADE). Experimental ADE measurements[8,16–34] and theoretical ADE calculations[10,35–46] both yield a broad range of values, although recent experimental and theoretical works converge to values around 1eV.[8–11,47] As indicated schematically in figure 1, the ADE is the minimal energy required to remove an electron from the SF_6^- anion ground state and produce ground state neutral SF_6. The experimental difficulty in SF_6^- ADE determination stems from the significant extension of the S-F bond length in the anion. The elongation of the S-F bond length from 1.56Å to 1.71Å results in a vanishing Frank-Condon (FC) overlap of the neutral and anion vibrational ground states, making it difficult to determine the ADE by directly observing a transition between the two states.[45] Also indicated in figure 1 are FC overlap factors between the anion ground state and vibrationally excited neutral states as a function of final state energy, recently determined based on an accurate large basis set CCSD(T) (coupled-cluster with single and double substitutions and perturbative account of triples) calculations of a C_{4v} distorted anion potential energy surface.[9,47,48] The calculated FC overlaps gradually increase with final state energy, from practically zero near the calculated 0.94eV ADE until the peak of the overlap at the vertical detachment energy (VDE) of ~4.2eV. Other theoretical works place the SF_6^- VDE in the 2.81-5.02eV range[44,46,49] while accepted experimental values are ~3eV as obtained by photoelectron spectroscopy (PES).[14] The recent high resolution PES studies on cold SF_6^- also showed surprising vibrational progressions and triggered theoretical calculations including breaking of the generally assumed O_h symmetry of the anion.[9] The photodetachment cross-section near the VDE region was measured experimentally in the 3.21-4.13eV region[50] as well as in the 3.18-3.46eV region,[51] reporting cross-sections as low as $8.1 \cdot 10^{-3}$Å^2 and $3 \cdot 10^{-4}$Å^2 at their respective measurement sensitivity limits. The later work estimated photodetachment (PD) threshold energy of 3.16eV based on a power threshold law fit of the measured cross section. However, the generally accepted recommended experimental ADE values are of about 1.03eV and are obtained indirectly by detailed modelling of the measured electron attachment and detachment kinetics.[21–24] Recent work revisiting the kinetic modeling[10] as well as new measurements of hot SF_6^- autodetachment lifetime[8] were inspired by improved theoretical calculation of the SF_6^- vibrational state density,[9] providing revised ADE estimates of 1.03eV and 0.91 eV respectively. It is interesting to note that the recommended experimental ADE values depend on our detailed modelling of the excited states of the SF_6^- anion, their creation by electron attachment and decay by auto

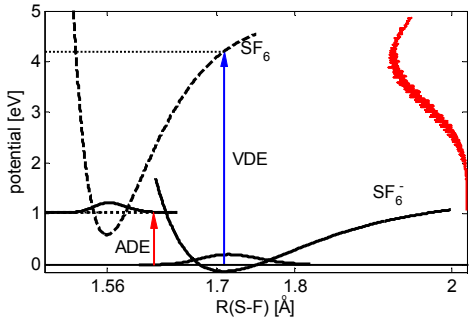

Figure 1: schematic SF_6 and SF_6^- potential curve shown respectively by the dashed and solid lines. Vibrational ground state functions are illustrated to emphasize the relativity large bind length shift and vertical arrows indicate the vertical and the adiabatic photodetachment processes. The red curve presents calculated relative FC overlaps of vibrationally excited neutral state with the anion ground state wave function, plotted as a function of photon energy.

detachment. Thus, complementary measurements of the detachment process near the ADE threshold are desirable.

In this work we extend the previously reported PD cross-section measurements performed near the VDE towards the ADE photon energy. Sensitive PD measurements, performed on cold SF_6^- anions in an electrostatic ion beam trap (EIBT),[52] allow recording the change of more than 4 orders of magnitude in the PD cross section reaching values as low as $2 \cdot 10^{-6}$Å^2 at photon energies below 2 eV. In the following we describe the sensitive measurement technique and discuss the extraction of experimental ADE values from the measured spectrum based on the calculated FC overlaps of the anion ground state with the low lying states of the neutral SF_6 molecule.

Experimental Scheme

Cold SF_6^- molecular anions formed in a pulsed supersonic expansion Even-Lavie ion source[53] are accelerated by 4.2keV potential and injected into a linear EIBT.[52] The fast ions are kept oscillating back and forth between two electrostatic mirrors, allowing us to isolate ions of specific charge over mass based on their oscillation frequency, interrogate them by tuneable wavelength laser and efficiently detect the neutral PD products. The main features of the EIBT setup are shown schematically in figure 2.

moving back and forth between the two mirrors.[55] The inset in figure 2 shows a typical capacitive pick-up signal of the synchronized passage of SF_6^- ions through a ring electrode located between the electrostatic mirrors, twice every oscillation cycle. The area of the negative peaks corresponds to the image charge induced on the pickup electrode and allows to determine the number of ions in the trapped ion bunch.[55,61] The non-destructive nature of the pickup measurement allows to continuously monitor the number of ions that interact with the PD laser and compensate for ion-source drifts during long measurement times. Furthermore, the off-center position of the pickup electrode serendipitously allows identifying the direction of the ion bunch motion towards or away from the MCP detector located downstream of the exit mirror. A deflector located in the field free region of the trap is used to implement the so called "kick-out" method,[56] used to isolate the SF_6^- ions by applying synchronized 100V pulses to the V_{KO} electrode that deflect undesirable ions such as SF_5^- and $(SF_6)_2^-$,oscillating out of synch with the applied pulses. A 10Hz tunable photodetachment OPO laser[62] is introduced through a dedicated 3mm hole in the MCP detector. The laser beam is overlapped co-linearly with the EIBT optical axis allowing efficient interrogation of the trapped ions. The 4ns laser pulses are timed in synch with the ion bunch direction to assure that neutral PD products continue in the parent ion path through the exit mirror and are detected on

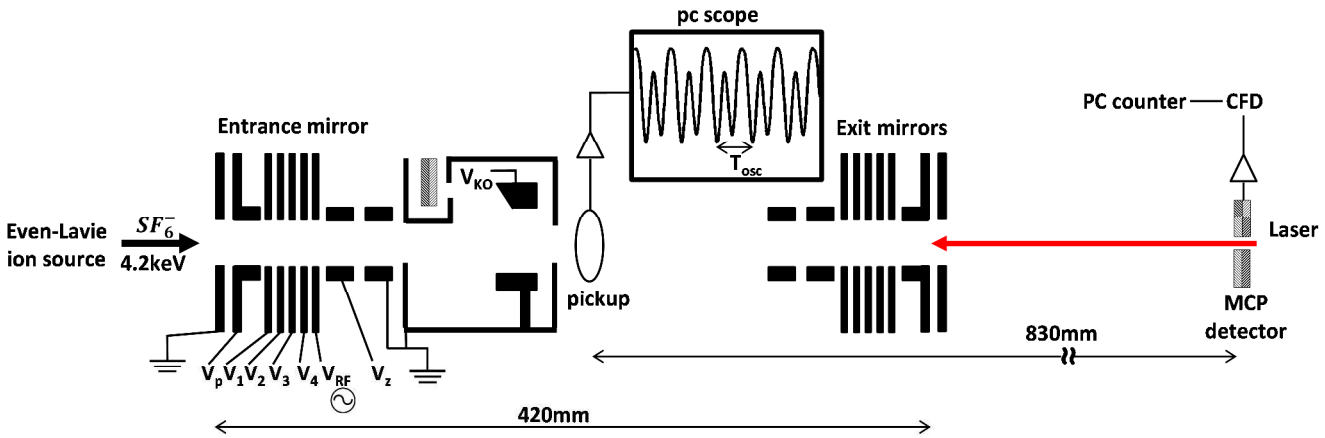

Figure 2: A schematic sketch of the EIBT setup. Cold SF_6^- formed in a pulsed ion source are accelerated and injected into the EIBT. The 4.2keV ion beam is stored between the entrance and exit electrostatic mirrors that are formed by a set of high voltage potentials (V_P = -4.42 kV, V_1 = -6.5kV, V_2 = -4.87 kV, V_3 = -3.25 kV, V_4 = -1.62 kV, V_z= -3.2 kV). The V_{RF} electrode is supplied with a ~4V RF potential to synchronize the SF_6^- oscillations in the trap. Synchronized HV pulses applied to the V_{KO} electrode deflect and remove undesirable ion masses from the EIBT. The pickup ring electrode is used to measure the number of trapped ions by recording their image charge on a PC-scope. Tunable wavelength OPO photodetachment laser is introduced through a hole in the neutral product MCP detector.

The EIBT and its applications were previously described in detail.[52,54–58] In this section we describe how the linear EIBT is used to perform high sensitivity PD cross section measurements. Ions are injected into the EIBT by lowering the potential on the entrance mirror electrode labelled V_P to allow ions of choice to enter the trap. Raising the V_P potential when ion at interest are inside the trap closes the EIBT and traps the ion beam. The typical residual gas pressure on the order of 10^{-10} torr in the EIBT region allows stable ion species to be trapped with lifetimes as long as 5 sec.[59] The PD efficiency measurements are all performed in the "normal diffusion" mode of the EIBT.[57,60] A low 4V RF voltage at the 87,062Hz oscillation frequency of SF_6^- ions is applied to the V_{RF} electrode in order to synchronize the motion of the ions of interest into a single ion bunch

the MCP detector. The well-defined geometry of the mass independent trapped ion trajectories are practically independent of potential ion source instabilities,[58] allowing reliable stable averaging of PD measurements over several days of measurement while continuously scanning laser wavelength in the 420-709nm signal and 210-419nm doubled frequency signal range of the OPO in steps of ~10meV.[62] In the following we demonstrate that PD cross sections on the order of 10^{-6}Å^2 can be recorded in this way, while maintaining sufficiently low laser flounce to avoid contributions from non-linear processes. Figure 3 shows a typical rate of neutral particle hits on the MCP as a function of trapping time, averaged of ~$2 \cdot 10^5$ injection cycles. The slowly decaying background signal is due to neutralization by collisions with the residual gas, while

the peaks at 25ms, 125ms and 225ms times correspond to neutral laser PD products.

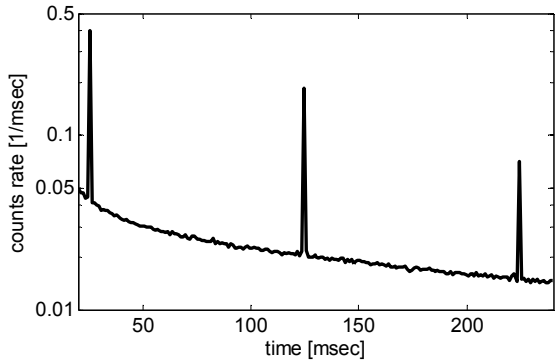

Figure 3: The neutral count rate, recorded by the MCP detector that is located after the EIBT and averaged over $\mathbf{2 \cdot 10^5}$ injection cycles. The three prominent peaks are due to the laser photodetachment signal.

Figure 4 shows a close-up view of the MCP count rate as a function of time from the laser pulse. The sharp peak at t=0 is due to electronic noise arriving in coincidence with the firing of the laser pulse. For SF_6^- parent ions, neutral photo detachment products born at the field free region in the center of the trap are expected to arrive in a time window between 8μs and 11.8μs after the laser pulse due to the time of flight from the EIBT to the MCP detector. Naturally the time of flight scales with the square root of the parent ion mass, allowing further cleaning, of the measured spectra from possible contaminations of the ion, performed in the data analysis stage. The small tail visible in the log scale representation is due to a negligible number of neutralization events that occur not in the field free region of the trap but inside the electrostatic mirror arriving with lower speed and therefore at slightly delayed time. The periodic background, which is 10^{-4} times smaller than the PD signal, is due to residual gas collisions and is modulated due to the oscillations of the ion bunch. As both PD and collision induced detachment products preserve the parent ion velocity, they arrive simultaneously to the detector. The trapped residual gas background count rate is averaged over 40 nearby

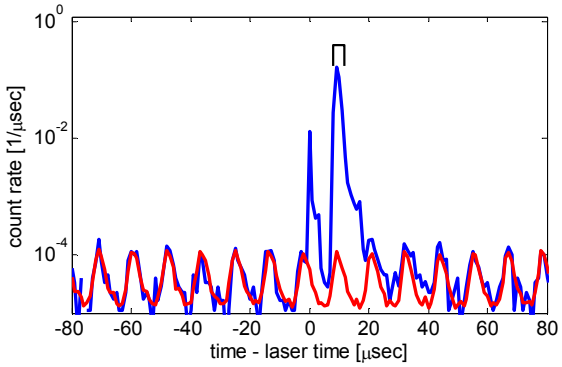

Figure 4: Solid blue line shows a close-up of the neutral count rate around the time of the first photodetachment laser shot. The sharp peak at time of the laser shot is due to electrical noise from the laser itself. The peak arriving at 8-11.7$\boldsymbol{\mu s}$ time corresponds to the neutral products of the ion-laser interaction that were produced in the center of the EIBT. The oscillatory background counts are due to the neutrals produced by collisions of the oscillating ions with the residual gas. The red solid line shows the subtracted background, estimated by averaging over 40 oscillations before and after the laser shot.

oscillations and subtracted from the counts arriving in coincidence with the laser to obtain the detected number of PD products.

In the low flux regime, the PD cross section is then calculated to be proportional to the detected number of products (N_{PD}) divided by the number of trapped ions measured by the pick-up electrode (N_{ions}) and photon flux(Φ), according to eq. 1:

$$(1) \quad \sigma_{PD}(h\nu) = \eta \frac{N_{PD}(h\nu)}{N_{ions}\,\Phi(\mathrm{h\nu})}$$

The proportionality constant η depends on the neutral detection efficiency and geometric laser-ion overlap factor.

Results and Discussion

The red lines in figure 5 show the measured PD cross section in the 1.94-2.91 and 3.62-4.28eV photon energy regions, corresponding to the signal and doubled frequency ranges of the OPO laser. As indicated in figure 3, PD measurements are repeated several times within each trapping cycle. We found no significant change in the measured PD cross sections as a function of trapping time (not shown). We conclude that within our spectral resolution, the possible anion temperature drift during the 250ms trapping time does not affect the presented PD cross section. The measured relative cross-section is scaled to fit the absolute ~0.02Å^2 cross section measured by Mock et al.[50] in the near VDE region, shown by the black squares in figure 5. In the VDE region the measured cross section changes slowly with photon energy, in agreement with Mock et al.[50] On the other hand, in the lower photon energy range the measured cross section exhibits a sharp drop by more than 4 orders of magnitude down to values of $1.6 \cdot 10^{-6}\text{Å}^2$, far below the noise levels of the previously reported measurements.[50,51] Including measurements of Datskos et al[51] that fall in the gap of the tunable OPO laser, preventing a direct comparison to the new data presented here. The monotonic increase of the measured cross section with increasing energy is in agreement with a direct detachment process, in which an electron is removed from the anion ground state is directly detached to produce excited vibrational states of the neutral SF_6. Indirect detachment, which can be mediated by favourable excited anion resonances, would result in resonance cross section structures that are not observed within our experimental resolution. We therefore compare the shape of the cross section drop to the expected cross section shape for the direct detachment mechanism, based on calculated FC overlaps of the initial anion state with the different neutral vibrational states.[9,47] The dashed blue line in figure 5 shows the shape of the calculated PD cross section. For every photon energy PD yield is estimated to be proportional to the sum over the FC overlaps of all energetically allowed final neutral states. In other words, all the states for which the sum of the neutral SF_6 vibrational energy and the ADE 0.94 eV, as calculated by Eisfeld et al,[9,47,48] is smaller than the respective photon energy. Although the dashed curve is arbitrarily scaled to fit the measured cross-section in the 2.8-2.9 eV range, it clearly exhibits a significantly slower cross-section drop compared to the measured data. It is valuable to note that the calculation uses the anion ground state, neglecting the thermal spread of the initial state. Nevertheless, the possible effect of a finite initial state temperature cannot account for the discrepancy with the experimental data as it would smear the cross section calculated for the anion ground state, resulting in yet milder rather than steeper cross section drop. Although we are not aware of favourable dissociative SF_6^- state, another possible cause for

differences between calculated and measured slopes could in principle be contribution from the energetically allowed $SF_5^- + F$ photodissociation channel.[23,24,46] However, neutral F atom products carry with them a low kinetic energy and are expected to have only few percent MCP detection probability. Furthermore, contribution from photodissociation is unlikely to account for the observed steep slope as an additional final channel

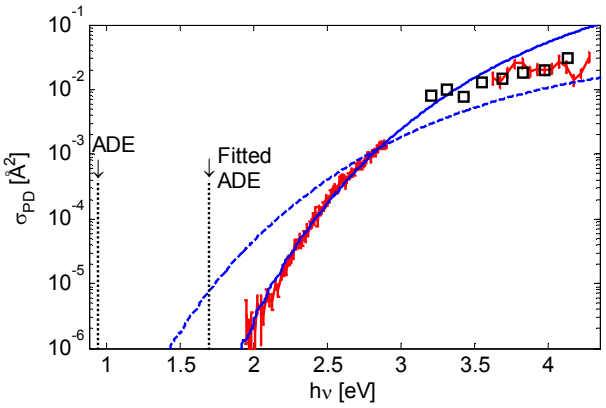

Figure 5: Solid red line shows the measured $\boldsymbol{SF_6^-}$ photodetachment cross section. Black squares indicate the previous absolute cross section measurement, performed by Mock et al.[50] in the VDE photon energy region. The dashed blue curve shows the shape of the section calculated based on the recently calculated Frank-Condon overlaps.[9] The solid blue line shows the calculated cross section, shifted according to the fitted ADE.

would smear rather than sharpen the observed threshold for neutral product appearance.

Calculation of molecular geometries and potential energy surfaces is often relatively more reliable than absolute ionization potentials and detachment energies. We therefore fit the data using the shape of the calculated PD cross section shape, while introducing an overall scaling factor and an ADE shift as free fit parameters. Assuming that the calculated FC overlaps can be reliable, even if the calculated absolute ADE is shifted. The best fit to the data shown by the solid blue line in figure 5 is obtained with a shift of 0.76 ± 0.02eV towards higher energies, corresponding to an ADE value of 1.7 eV. The evident agreement with the measured data persists remarkably over 1 eV and several orders of magnitude cross section change. Although the calculated curve overshoots the measured cross section at the VDE region, possibly reflecting the higher calculated VDE value compared to experimental VDE determination, the overall increase of 4 orders of magnitude is well reproduced. The measured curve shape could not be well represented by fitting with simple threshold Wigner threshold law often used in analysis of near threshold photoionization and PD data.[63,64] Interestingly, a $\sigma_{PD} \propto (1 - ADE/h\nu)^{1/2}$ phenomenological threshold law sometimes applied in astrophysics[65] successfully fits the data below 3 eV with an ADE = 1.7 ± 0.02 eV. The fitted phenomenological threshold law curve is not shown as it practically indistinguishable from the calculated blue solid curve in figure 5. Fitting the measured PD data with either the calculated FC overlaps or with the phenomenological threshold law results with ADE values of 1.7 ± 0.02 eV that are considerably higher than the recommended experimental values at about 1eV.[9,47] Indeed, the steep PD cross section drop combined with the reduced OPO laser power at the lower photon energies prevented a direct measurement of the inefficient PD transition to the vibrational ground state at ADE photon energy. Nevertheless, the agreement over several orders of magnitude between the measured data and the calculated cross-section is remarkable. We note again that the recommended experimental values rely on our modelling of electron attachment to form excited anion states as well as on the decay of excited anions due to autodetachment.[66] particularly the decay probabilities of highly excited rovibrational anion states, modelled based on high accuracy calculations of rotationally cold a-symmetric SF_6^- system, play an important role in ADE estimation.[8,10] In contrast, ADE extraction from PD data as presented here requires high accuracy modelling of the low lying vibrational states of the symmetric neutral SF_6 system and of the anion ground state that are in principle less challenging theoretically.[9,47] Furthermore, interpretation of both experimental approaches could be in principle affected by indirect mechanisms for electron attachment or detachment via resonances, mediated by electronically excited SF_6^- states.[46,66–68]

Conclusions

Photodetachment measurements of cold SF_6^- anions were performed using an EIBT, allowing highly sensitive measurements of PD cross sections on the 10^{-6}Å² scale. The measured PD cross section was extended by more than an eV towards lower photon energies, approaching the ADE threshold limit. Fitting the measured shape of the steep cross section drop more than 3 orders of magnitude with either a phenomenological threshold law function,[65] or with previously calculated FC overlaps,[47] allows extraction of SF_6^- ADE values of 1.7 ± 0.02 eV, significantly higher than the presently accepted experimental estimates that are based on electron attachment and electron detachment kinetics modelling.[10] As both experimental approaches rely on theoretically calculated inputs in order to extract ADE values, we propose that further theoretical work is required to resolve the apparent discrepancy. For example, by providing improved SF_6^- anion vibrational ground state wave function calculation in the overlap region that accounts for the observed steep cross section drop, while maintaining lower ADE. Or alternatively by providing theoretical description of either bound or dissociative excited anion states that may alter the interpretation of the experimental data.

Notes and references

[a] Institute of Chemistry, The Hebrew university of Jerusalem, Jerusalem, 91904, Israel.
[b] Department of Particle Physics, Weizmann Institute of Science, Rehovot, 76100, Israel.

1. L. G. Christophorou and J. K. Olthoff, *J. Phys. Chem. Ref. Data*, 2000, **29**, 267.
2. J. T. Houghton, M. L. G. Filho, B. A. Callander, N. Harris, A. Kattenberg, and K. Maskell, *Climate Change 1995*, 1996.
3. R. A. Morris, T. M. Miller, A. A. Viggiano, J. F. Paulson, S. Solomon, and G. Reid, *J. Geophys. Res.*, 1995, **100**, 1287–1294.
4. T. Reddmann, R. Ruhnke, and W. Kouker, *J. Geophys. Res.*, 2001, **106**, 14525.

5. K. W. K. Malcolm, N. D. Sze, W.-C. Wang, G. Shia, A. Goldman, F. j. Murcray, D. G. Murcray, and C. P. Rinsland, *J. Geophys. Res.*, 1993, **98**, 10,499–10,507.

6. M. Braun, S. Marienfeld, M.-W. Ruf, and H. Hotop, *J. Phys. B At. Mol. Opt. Phys.*, 2009, **42**, 125202.

7. Y. Albeck, D. M. Kandhasamy, and D. Strasser, *J. Phys. Chem. A*, 2014, **118**, 388–95.

8. S. Menk, S. Das, K. Blaum, M. W. Froese, M. Lange, M. Mukherjee, R. Repnow, D. Schwalm, R. von Hahn, and a. Wolf, *Phys. Rev. A*, 2014, **89**, 022502.

9. W. Eisfeld, *J. Chem. Phys.*, 2011, **134**, 054303.

10. J. Troe, T. M. Miller, and A. A. Viggiano, *J. Chem. Phys.*, 2012, **136**, 121102.

11. A. Karton and J. M. L. Martin, *J. Chem. Phys.*, 2012, **136**, 197101.

12. L. H. Andersen, *Phys. Rev. A*, 2008, **78**, 032512.

13. W. R. Johnstone and W. M. Newell, *J. Phys. E At. Mol. Opt. Phys.*, 1991, **24**, 473–487.

14. J. C. Bopp, J. R. Roscioli, M. A. Johnson, T. M. Miller, A. A. Viggiano, S. M. Villano, S. W. Wren, and W. C. Lineberger, *J. Phys. Chem. A*, 2007, **111**, 1214–1221.

15. J. Rajput, L. Lammich, and L. H. Andersen, *Phys. Rev. Lett.*, 2008, **100**, 153001.

16. R. N. Compton, G. L. Christophorou, G. S. Hurst, and P. W. Reinhardt, *J. Chem. Phys.*, 1966, **45**, 4634.

17. E. Chen, R. D. George, and W. E. Wentworth, *J. Chem. Phys.*, 1968, **49**, 1973.

18. F. C. Fehsenfeld, *J. Chem. Phys.*, 1971, **54**, 438.

19. R. N. Compton, P. W. Reinhardt, and C. D. Cooper, *J. Chem. Phys.*, 1978, **68**, 2023.

20. G. E. Streit, *J. Chem. Phys.*, 1982, **77**, 826.

21. E. P. Grimsrud, S. Chowdhury, and P. Kebarle, *J. Chem. Phys.*, 1985, **83**, 1059.

22. E. C. M. Chen, J. R. Wiley, C. F. Batten, and W. E. Wentworth, *J. Phys. Chem.*, 1994, **98**, 88–94.

23. A. A. Viggiano, T. M. Miller, J. F. Friedman, and J. Troe, *J. Chem. Phys.*, 2007, **127**, 244305.

24. J. Troe, T. M. Miller, and A. a. Viggiano, *J. Chem. Phys.*, 2007, **127**, 244304.

25. C. Lifshitz, T. O. Tiernan, and B. M. Hughes, *J. Chem. Phys.*, 1973, **59**, 3182.

26. R. N. Compton and C. D. Cooper, *J. Chem. Phys.*, 1973, **59**, 4140.

27. M. M. Hubers and J. Los, *Chem. Phys.*, 1975, **10**, 235–259.

28. K. M. A. Refaey and J. L. Franklin, *Int. J. Mass Spectrom. Ion Phys.*, 1978, **26**, 125–130.

29. M. W. Chase, J. L. Curnutt, J. R. Downey, R. A. McDonald, A. N. Syverud, and E. A. Valenzuela, *J. Phys. Chem. Ref. Data*, 1982, **11**, 695.

30. P. S. Drzaic and J. I. Brauman, *Am. Chem. Soc.*, 1982, **104**, 13–19.

31. S. P. Heneghan and S. W. Benson, *Int. J. Chem. Kinet.*, 1983, **15**, 109–117.

32. E. C. M. Chen and W. E. Wentworth, *J. Phys. Chem.*, 1983, **87**, 45–49.

33. C. Lifshitz, *J. Phys. Chem.*, 1983, **87**, 3474–3479.

34. E. C. M. Chen, L.-R. Shuie, E. Desai D'sa, C. F. Batten, and W. E. Wentworth, *J. Chem. Phys.*, 1988, **88**, 4711.

35. G. L. Gutsev and R. J. Bartlett, *Mol. Phys.*, 1998, **94**, 121–125.

36. G. L. Gutsev, *Int. J. Mass Spectrom. Ion Process.*, 1992, **185**, 185–192.

37. K. W. Richman and A. Banerjee, *Int. J. Quantum Chem.*, 1993, **767**, 759–767.

38. C. W. Bauschlicher and A. Ricca, *J. Phys. Chem. A*, 1998, **5639**, 4722–4727.

39. M. Boring, *Chem. Phys. Lett.*, 1977, **46**, 242–244.

40. P. Jeffrey Hay, *J. Chem. Phys.*, 1982, **76**, 502.

41. R. Tang and J. Callaway, *J. Chem. Phys.*, 1986, **84**, 6854.

42. M. Klobukowski, Z. Barandiarán, L. Seijo, and S. Huzinaga, *J. Chem. Phys.*, 1987, **86**, 1637.

43. E. Miyoshi, Y. Sakai, and S. Miyoshi, *J. Chem. Phys.*, 1988, **88**, 1470.

44. R. A. King, J. M. Galbraith, and H. F. Schaefer III, *J. Phys. Chem*, 1996, **100**, 6061–6068.

45. R. Borrelli, *Chem. Phys. Lett.*, 2007, **445**, 84–88.

46. A. F. Jalbout, A. De Leon, L. Adamowicz, B. Trzaskowski, E. C. M. Chen, C. Herder, and E. S. Chen, *J. Theor. Comput. Chem.*, 2007, **6**, 747–759.

47. W. Eisfeld, *J. Chem. Phys.*, 2011, **134**, 129903.

48. E. Wolfgang, *private communication*, 2014.

49. G. L. Gutsev and R. J. Bartlett, *Mol. Phys.*, 1998, **94**, 121–125.

50. R. S. Mock and E. P. Grimsrud, *Chem. Phys. Lett.*, 1991, **184**, 99–101.

51. P. G. Datskos, J. G. Carter, and L. G. Christophorou, *Chem. Phys. Lett.*, 1995, **239**.

52. D. Zajfman, O. Heber, L. Vejby-Christensen, I. Ben-Itzhak, M. Rappaport, R. Fishman, and M. Dahan, *Phys. Rev. A*, 1997, **55**, R1577–R1580.

53. U. Even, J. Jortner, D. Noy, N. Lavie, and C. Cossart-Magos, *J. Chem. Phys.*, 2000, **112**, 8068.

54. O. Aviv, B. Kafle, V. Chandrasekaran, O. Heber, M. L. Rappaport, H. Rubinstein, D. Schwalm, D. Strasser, Y. Toker, and D. Zajfman, *Rev. Sci. Instrum.*, 2013, **84**, 053106.

55. I. Rahinov, Y. Toker, O. Heber, D. Strasser, and M. Rappaport, *Rev. Sci. Instrum.*, 2012, **83**, 033302.

56. Y. Toker, N. Altstein, O. Aviv, M. L. Rappaport, O. Heber, D. Schwalm, D. Strasser, and D. Zajfman, *J. Instrum.*, 2009, **4**, P09001.

57. D. Strasser, T. Geyer, H. Pedersen, O. Heber, S. Goldberg, B. Amarant, a. Diner, Y. Rudich, I. Sagi, M. Rappaport, D. Tannor, and D. Zajfman, *Phys. Rev. Lett.*, 2002, **89**, 283204.

58. D. Attia, D. Strasser, O. Heber, M. L. Rappaport, and D. Zajfman, *Nucl. Instruments Methods Phys. Res. Sect. A Accel. Spectrometers, Detect. Assoc. Equip.*, 2005, **547**, 279–286.

59. H. Pedersen, D. Strasser, O. Heber, M. Rappaport, and D. Zajfman, *Phys. Rev. A*, 2002, **65**, 042703.

60. H. Pedersen, D. Strasser, B. Amarant, O. Heber, M. Rappaport, and D. Zajfman, *Phys. Rev. A*, 2002, **65**, 042704.

61. O. Heber, P. D. Witte, a. Diner, K. G. Bhushan, D. Strasser, Y. Toker, M. L. Rappaport, I. Ben-Itzhak, N. Altstein, D. Schwalm, a. Wolf, and D. Zajfman, *Rev. Sci. Instrum.*, 2005, **76**, 013104.

62. EKSPLA, *Tunable Nd:YAG-Laser System NT342B-SH*, .

63. E. P. Wigner, *Phys. Rev.*, 1948, **73**, 1002.

64. J. W. Farley, *Phys. Rev. A*, 1989, **40**, 6286.

65. T. J. Millar, C. Walsh, M. A. Cordiner, R. N. Chuimın, and E. Herbst, *Astrophys. J.*, 2007, **662**, 87–90.

66. G. L. Gutsev, *Inst. Chem. Physics, Russ. Acad. Sci.*, 1992, **5622**, 504–510.

67. S. Avrillier and J.-P. Schermann, *Opt. Commun.*, 1976, **19**, 87–91.

68. E. C. M. Chen and E. S. Chen, *Phys. Rev. A*, 2007, **76**, 032508.

